

Implementation and analysis of 5G network identification operations at low signal-to-noise ratio

Ilya Pyatin¹, Juliy Boiko², Oleksander Eromenko³, Igor Parkhomey⁴

¹Department of Computer Engineering, Faculty of Computer Engineering, Khmelnytskyi Polytechnic Professional College by Lviv Polytechnic National University, Khmelnytskyi, Ukraine

²Department of Telecommunications, Media and Intelligent Technologies, Faculty of Information Technologies, Khmelnytskyi National University, Khmelnytskyi, Ukraine

³Department of Physics and Electrical Engineering, Faculty of Information Technologies, Khmelnytskyi National University, Khmelnytskyi, Ukraine

⁴Department of Software Engineering, Faculty of Cybersecurity, Computer and Software Engineering, National Aviation University, Kyiv, Ukraine

Article Info

Article history:

Received Jan 14, 2022

Revised Apr 12, 2022

Accepted Dec 28, 2022

Keywords:

5G mobile networks

Correlation

OFDM

Signal-to-noise ratio

Synchronization

ABSTRACT

The article investigates the operations of identifying a cellular network and searching for a cell at various signal-to-noise ratios. The estimation of frequency and time displacement, criteria for detecting the primary synchronization signal are presented. The main contribution of this article is the consideration of the step-by-step execution of the 5G cell search procedure in a complex interference environment. The decoding steps of the primary and secondary synchronization signals are being investigated. This is achieved by analyzing the signals at each step of the correlation algorithm for different signal-to-noise ratios. In order to verify the adequacy of the proposed models, a sequence operation for synchronizing 5G mobile networks with base station signals is considered. The dependence of the magnitude of the error vector modulus on the signal-to-noise ratio of a physical broadcasting channel is investigated for three different channel profiles without line of sight. As a result of the experiment, the error vector of the physical broadcast channel changes from 55% to 10%, when the signal-to-noise ratio changes from 0 to 20 dB. In the multiple-input multiple-output (MIMO) mode, we received a 3 dB increase in communication energy efficiency. The findings will be useful for 5G system designers to troubleshoot synchronization problems.

This is an open access article under the [CC BY-SA](https://creativecommons.org/licenses/by-sa/4.0/) license.



Corresponding Author:

Juliy Boiko

Department of Telecommunications, Media and Intelligent Technologies

Faculty of Information Technologies, Khmelnytskyi National University, Khmelnytskyi, Ukraine

Email: boiko_julius@ukr.net

1. INTRODUCTION

The 5G standard uses high carrier frequencies. Such frequencies lead to large values of frequency and time offsets [1]. To reduce interference, in the case of information transmission, it is necessary to have an accurate generator when setting up the transmitter and receiver. Interference sources are mainly associated with the disadvantages of orthogonal frequency division multiplexing (OFDM) systems [2], [3]. In such systems, time and frequency offsets occur, resulting in inter-symbol interference (ISI) and inter-subcarrier interference (ICI). The transmitted signal reaches the receiver with a time delay. The receiver does not know when the transmitter has sent a new packet. Typically, a normalized time offset is considered, equal to the number of samples between the transmitted and received signals. If the normalized time offset is greater than

the length of the cyclic prefix (CP), there may be a fast Fourier transform (FFT) window inconsistency. Autocorrelation and cross-correlation algorithms are well known in the literature [4] and are used in wireless communication systems. In the first algorithm, the received signal is correlated with a delayed version of the same signal. In the second algorithm, the received signal is correlated with a stored pattern known to the receiver. In addition to timing offset, errors in the transmitter and receiver oscillators lead to frequency offset. Unlike a time shift, this phase shift increases with time because it is directly proportional to the discrete time index. The frequency offset in OFDM is usually normalized to the interval between subcarriers. The relationship between the frequency error and the inter-subcarrier spacing is used. In addition, the discrepancy between the sampling rate at both the transmitter and receiver is another source of time bias.

In the literature [5], [6], a description of numerology, signals and the procedure for achieving synchronization is given, but the dependence of the inter-correlation functions of the primary synchronization signal (PSS) at low signal-to-noise ratios (SNR) and on skip of synchronization is not investigated. In [7], [8] there is also no estimate of the shifts in the time and frequency domains that occur at low SNR and at the synchronization skip. Youssif *et al.* [9] it is shown that if the sampling rates on the transmitting and receiving sides of the OFDM channel are out of phase, a symbol synchronization error occurs, which can generally be attributed to clock synchronization errors. In this case, the samples on the receiving side differ from the samples on the transmitter side, a phase shift occurs and, as a consequence, the sampling times of the receiver and the transmitter do not coincide [10]. In this situation, a certain time delay occurs on the receiving side due to the deviation of the samples from the optimal values. This process is accompanied by a phase offset that is proportional to the timing offset and subcarrier indices [11]-[13]. The timing error can be caused by a mismatch between the transmitter and receiver frequencies due to Doppler shift resulting in intersymbol interference between the OFDM carriers. In particular, the physical level of organization of synchronization in 5G technology is described in [14], [15]. Soatti *et al.* [15], aspects of node-to-node synchronization of 5G in the context of the implementation of Internet of Things technologies are considered in detail. In [16]-[22] general concepts organization synchronization systems and design of detectors synchronization errors are considered, provided that multi-position modulation signals are used [23]-[25]. Fourati *et al.* [26] considers modern concepts for self-organizing cellular networks applied to 5G. Evaluation of the impact of ISI on the quality of OFDM signal processing is considered in [27]. Promising antenna systems for 5G are considered in Mattered and Tanda [28], the problems of network optimization and coding in them are studied in the articles [29], [30]. However, the issues of network identification were not discussed.

The proposed work complements the research of the mentioned authors. The article presents the study of signals mobile telecommunications in extreme conditions in the presence and absence of synchronization the mobile subscriber with the base station. Such information is needed to debug the operation of mobile telecommunications in difficult urban environments with random jumps in the signal level, topographic features of the terrain. Signal strength is negatively impacted by trees, hills, buildings, weather and other obstacles.

2. RESEARCH METHOD

In this section describes a waveform algorithm that contains a signal synchronization burst (SS), transmit the wave over a channel with AWGN, and then synchronization to the received waveform to decode the master information block (MIB). An algorithm of cross-correlation synchronization using primary synchronization signal (PSS) is considered. Mathematical description and concepts of m -sequence PSS for 5G technology are presented.

2.1. Synchronization of customer equipment with base station signals

The concept of user equipment entering the network for the purpose of exchanging data involves the steps involved in finding and selecting a cell. In addition, it is necessary to provide conditions for obtaining system information of the primary type. Thus, it is important to ensure the conditions for synchronizing the corresponding frames, it is necessary to carry out the process of identifying the type of cellular network. Along with the synchronization process, the decoding order of the main information block is also organized. The general structure of the model of the synchronization system for research is shown in Figure 1.

In Figure 2 shows the strategy of the synchronization process in 5G NR in the form of a flowchart. The refinement of this process is based on principles where the gNode base station (gNB) uses a beam sweep and periodically emits a timing synchronization signal in a burst form (SSB). This signal contains several SSBs and is characterized by the following frequency $T_{SS} = \{5, 10, 20, 40, 80, 160\}$ ms.

For the primary access form in the standby mode, the user equipment starts the process of searching for a network cell. In this mode, the user equipment starts the PSS and second synchronization (SSS) timing procedures, evaluates and corrects the required frequency and time offset. In this case, the following features should be noted when the PSS is for identifying a primary symbol in a sync frame while the SSS is for identifying a primary symbol in a subframe.

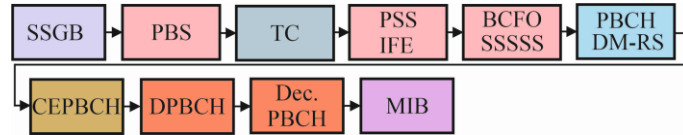


Figure 1. Synchronization study model structure

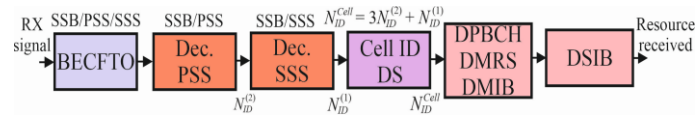


Figure 2. Signal processing circuitry for synchronization in 5G

On Figure 1 we used the following notation where SSGB is the synchronization signal generation unit in burst form; PBS is the unit that provides a beam scan; TC is the transmission channel. We have also used the following notation for channel block blocks and correction blocks: PSS IFE is the primary synchronization signal and initial frequency estimate; BCFO SSSSS is the block for fine correction of frequency offset and secondary synchronization signal search system; PBCH DM-RS is the broadcast physical channel and demodulation reference signal; CE PBCH is the channel state estimation unit using a physical broadcasting channel. To designate the demodulation and decoding blocks, we used the following designations: DPBCH is the demodulation a physical broadcasting channel; Dec. PBCH is the decoding a physical broadcasting channel; MIB is the main information block.

In the scheme presented in Figure 2 we used the following notation. For blocks responsible for estimating and correcting - BECFTO is the block for estimating and correcting frequency and time offset. The set of blocks of primary and secondary decoding, as well as detection, are marked respectively as Dec. PSS is the decoding of a primary synchronization signal; Dec. SSS is the decoding of a second synchronization signal; cell ID DS is the cell ID detection system. We marked the components responsible for the reference signal and system information respectively as DPBCH DMRS DMIB is the decoding unit for demodulation reference signal and main information unit; DSIB is decoding the system information block.

Carrying out the decoding process of the primary sync block allows the user to discover the network ID ($N_{ID}^{(2)}$). Further, according to the scheme in Figure 2, using $N_{ID}^{(2)}$, the user performs decoding of the secondary signal and detects already a group of cell identifiers $N_{ID}^{(1)}$. It is important that the service cell ID is calculated here, which can be represented by an expression: $N_{ID}^{Cell} = 3N_{ID}^{(2)} + N_{ID}^{(1)}$.

Determining the network identifier allows the user to identify the sync packet in the general structure of the SS sync frame. In the OFDM concept, sub-carrier spacing generally uses a specific set of SSB sync packets, each marked with a separate index of the first symbols in the half-frame structure. Thus, each SSB sync burst will characterize the corresponding beam. In such a case, in order to find the index of the serving beam, the user must identify the corresponding SSB ($0, 1, 2, \dots, L - 1$). In practice, this means that after receiving the PBCH signal, the user must define two ($L = 2$) or three ($L > 4$) significant bits for the SBB sync packet. So, the user sets the sampling time and frame number (SFN). Then, if the decoding of the MIB is done successfully, the SFN will become known.

Summarizing the above in the text, we focus on the following. For initial access or idle mode, it is common for beam steering to apply PSS, SSS, and the DM-RS procedure. In this context, the implementation of the cell search process is a critical step to ensure synchronization in 5G NR. The main purpose of such a process is to accurately correct and eliminate time and frequency errors.

2.2. Stages of signal processing in the synchronization system

Let's consider the main stages of signal processing in the system. The content of the SS structure is characterized by the placement of the SS/PBCH block template in the overall package construction and the placement of the already mentioned MIB. We represent the design of the transmission channel as a tapped delay line (TDL) with the ability to add white Gaussian noise (AWGN) and the ability to affect the SNR [24].

In the case of packet creation, a set of OFDM signal resources with the contents of the SS packets is formed. The formation of the volume of the resource grid is carried out in such a way that the modulated OFDM signal receives a sampling frequency of such a value, which is convenient to integrate into the PDCCH and PDSCH carrier signal. In Figure 3, we present the resulting structure of the resource grid, which includes SS packages. Combining signals in the time domain is required if the SS/PBCH block and PDCCH-PDSCH have different subcarrier placement steps.

The unfolding of the grid in the OFDM signal resource for the SS packet implementation is performed by beamforming the transmitter antenna. The peculiarity of this process is that each block of the SS-PBCH type in the packet interpretation is implemented by a separate vector of the generated radiation pattern. Next, the OFDM resource grid is modulated to obtain a signal in the time domain. For a visual representation of the principles of forming OFDM symbols corresponding to the SS packet and the concept of gridding for beam generation, Figure 4.

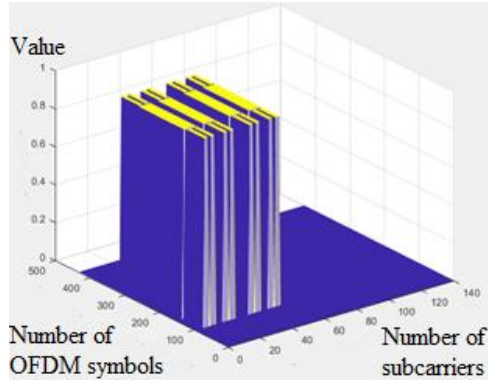


Figure 3. Resource grid device containing SS burst

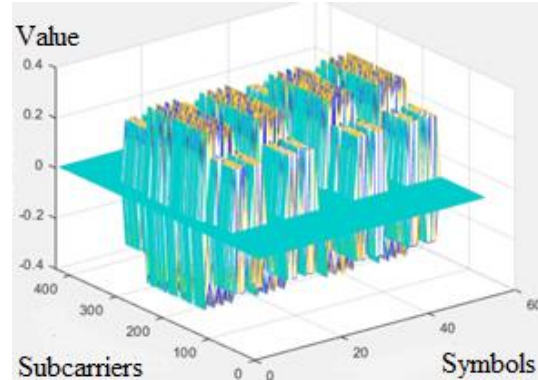


Figure 4. Resource gridding for beam generation

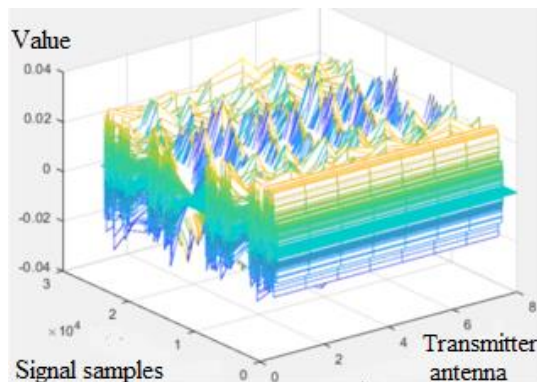


Figure 5. Transmitter waveform

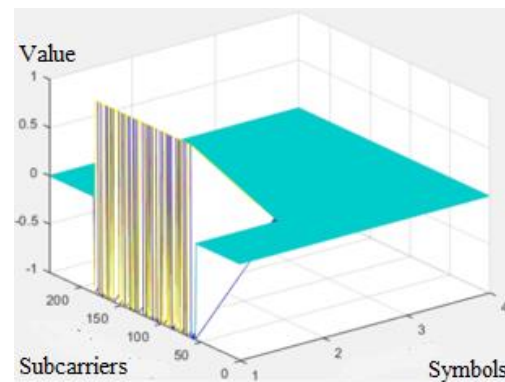


Figure 6. Visualization of the generated grid of PSS resources

In Figure 5 shows an image of a synthesized wave from a radio transmitter. The generated signal was fed to the model of the transmission channel in the form of TDL and thus the signal for the configured number of antennas was generated. The AWGN model was used. The resulting construction reflecting the PSS resource grid is shown in Figure 6.

When a signal arrives at the input of the receiver, a PSS search is performed. To do this, we apply correlation processing of the received signal (taking into account all blocks of the SS-PBCH type) with three possible constructions of the PSS-type sequences. The end action of this signal processing is to identify the peak with the highest correlation value. Thus, determining the SS/PBCH block with the highest correlation allows you to determine which of the beams used in the sweep is the most efficient in the transmitter-receiver configuration. The use of frequency offset hypotheses is used to initially estimate the received signal. Adjustments for a specific offset are made by determining the highest correlation. The next step is to fine-tune the frequency reduction, determine the SSS, and search for a reference signal.

During PBCH demodulation, the channel and noise level are estimated to correct the mean square error (MSE). The corrected PBCH symbols after demodulation are used to estimate the bit structure in the code block. Let's describe the synchronization signals. We use PSS and SSS to fix the borders of the radio frame and set the cell identifier. 5G NR technology has the following structure, when a single cell contains 1008 identifiers included in 336 groups ($N_{ID}^{(1)} \in \{0, \dots, 355\}$). Groups contain sectors ($N_{ID}^{(2)} \in \{1, 2, 3\}$). When installing PSS and SSS, the user calculates the cell identifier by:

$$N_{ID}^{(2)} = 3N_{ID}^{(1)} + N_{ID}^{(2)} \quad (1)$$

The PSS structure for 5G NR consists of an m -sequence which is formed by a feedback shift register. This signal contains 127 active subcarriers. The construction of an m -sequence can be represented [1].

$$d_{PSS}(n) = 1 - 2x(m) \quad (2)$$

Where:

$$m = (n + 43N_{ID}^{(2)}) \bmod 127,$$

$$(0 \leq n < 127); [x(6)x(5)x(4)x(3)x(2)x(1)x(0)] = [11101110].$$

The SSS type signal in 5G is used to set the cell ID groups ($N_{ID}^{(1)}$). Its design contains 336 sequences, 127 symbols each, and is mapped to the 3rd SSB symbol on 127 subcarriers. Mathematically, SSS sequences can be represented (3).

$$d_{SSS}(n) = [1 - 2x_0((n + m_0) \bmod 127)][1 - 2x_1((n + m_1) \bmod 127)] \quad (3)$$

Where:

$$m_0 = 15 \left\lfloor \frac{N_{ID}^{(1)}}{112} \right\rfloor + 5N_{ID}^{(2)}; m_1 = N_{ID}^{(1)} \bmod 112, (0 \leq n \leq 127);$$

$$[x_0(6)x_0(5)x_0(4)x_0(3)x_0(2)x_0(1)x_0(0)] = [0000001];$$

$$[x_1(6)x_1(5)x_1(4)x_1(3)x_1(2)x_1(1)x_1(0)] = [0000001].$$

We noted that correlation weighting is applied in the synchronization process. To proceed to modeling correlation processing during synchronization, note the following. Therefore, the received signal is correlated with the stored PSS pattern known at the receiving side. Consider this cross-correlation for the following reasons. Let us describe the mathematically received signal by (4).

$$r(n) = s(n) \otimes h(n) + \xi(n) \quad (4)$$

Where $s(n)$ is the transmitted signal, $h(n)$ is the channel impulse response, $\xi(n)$ is the noise component, and \otimes is the linear convolution operator. The received signal in the presence of the phenomenon of carrier frequency offset can be represented by:

$$r_\mu(n) = [s(n) \otimes h(n) + \xi(n)] e^{j\frac{2\pi n}{N_{FFT}}\mu} \quad (5)$$

Where μ is the normalized frequency offset, consisting of an integer and fractional part.

Let us define the results of evaluating the PSS synchronization system as $\hat{\delta}$. Let us denote the result of evaluating the network identification procedure as $\hat{\nu} \in \{0,1,2\}$. Then, based on the available received signal presented in the time domain, we establish the criterion for the overall assessment ($\hat{\delta}$ and $\hat{\nu}$) of the synchronization process:

$$(\hat{\delta}, \hat{\nu}) = \arg \max_{\delta, \nu} (C(\delta, \nu)) \quad (6)$$

Where $C(\delta, \nu)$ is the cross-correlation determined by [1]:

$$C(\delta, \nu) = \frac{|\sum_{l=0}^{N_{FFT}-1} r(\delta+l)p_\nu^*(l)|}{\sum_{l=0}^{N_{FFT}-1} |r(\delta+l)|^2}, \quad (7)$$

Where $r(\delta + l)$ is used the designation describing the delayed signal; $p_i^*(l)$ describes PSS-signal sequence for the time domain in the network ν identification sector; N_{FFT} defines the digit capacity of the FFT (the CP is not taken into account). An expression can then be used to estimate the frequency error when inter-frequency interference occurs. In this case, the carrier frequency offset can be estimated taking into account integral and fractional frequency shifts.

You can also consider an autocorrelation synchronization algorithm using CP. In this case, the autocorrelation of a part of the received signal with the corresponding part of CP is determined. The main idea of such an algorithm. Let's designate the value of correlation and energy $\gamma(\delta)$, $\alpha(\delta)$ respectively, then we analytically represent them:

$$\gamma(\delta) = \sum_{l=0}^{\delta+L-1} r(l)r \times (l + N_{FFT}) \quad (8)$$

$$\alpha(\delta) = \sum_{l=0}^{\delta+L-1} |r(l)|^2 + |r(l + N_{FFT})|^2 \quad (9)$$

Where L is the length of CP. Then the estimation of the error can be carried out on the basis of maximum likelihood [24].

$$\hat{\delta} = \max(2|\gamma(\delta)| - \rho L(\delta)) \quad (10)$$

$$\hat{\mu} = -\frac{1}{2\pi} L(\gamma(\hat{\delta})) \quad (11)$$

Where ρ is the value of the correlation coefficient between $r(l)$ and $r(l + N)$ represented by:

$$\rho = \frac{\sigma_S^2}{\sigma_S^2 + \sigma_N^2} \quad (12)$$

Where σ_S^2, σ_N^2 is the spectral power of signal and noise.

Summarizing the analysis performed, it can be noted that the accuracy of the described methods can be improved by averaging the estimates of time and frequency offsets over several OFDM symbols. However, the use of the autocorrelation method does not allow the determination of the cell identifier. In general, the coarse frequency offset can be estimated from the PSS offset, while small errors are estimated using autocorrelation as will be presented in the experimental section below. Thus, the estimation and correction of the time-frequency offset is an important task in the general procedure for synchronizing mobile telecommunications.

3. RESULTS AND DISCUSSION

In this section, it displays the results of a 5G mobile telecommunications signal synchronization study. Experimental studies on the estimation of the root-mean-square (RMS) value of the magnitude of the error vector (EVM) are presented, recommendations are given for correcting coarse and fine errors in identifying the frequency shift when using a synchronization system. The influence of the SNR level on the qualitative indicators of the synchronization system actuation has been clarified.

3.1. Investigation of synchronization conditions based on the correlation estimate

To synchronize the waveform in time, we use a method that is based on the estimate of the PSS time offset with the highest correlation. An increase in the accuracy of the synchronization error estimate was carried out based on the determination of the degree of correlation [16] between the CP OFDM symbols in SSB and the payload of the OFDM symbol sequence. Because coarse and residual timing estimates have conflicting characteristics, we considered a hybrid design that included both coarse and fine timing estimates.

Simulation parameters: symbol rate = 15.36 Msamp/s; cell ID = 102. In Figure 7 is a plot of PSS correlation versus frequency offset when SNR = 15 dB. The correlation of SSS symbols on the receiver for SNR = 15 dB is shown in Figure 8.

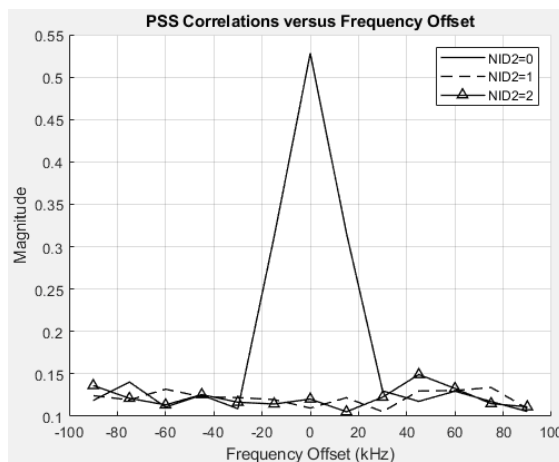


Figure 7. Graphical correlation estimates of PSS versus frequency change (SNR = 15 dB)

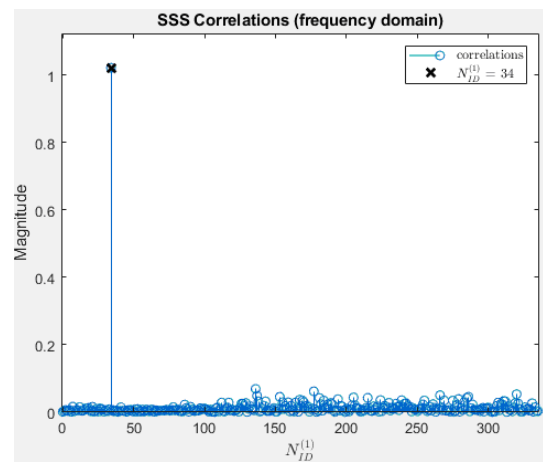


Figure 8. SSS correlation at the receiver (SNR = 15 dB)

The estimation process consisted of PSS search, correlation estimation of the transmitted signal shape (estimation was performed on all SS/PBCH blocks). The degree of correlation was determined for three PSS probable sequences with the establishment the most significant peak correlation value. The result of this approach is to identify the SS/PBCH with peak correlation and identify the beam that was most efficient for the link between the transmitter and receiver. We received the reference signal while modulating the OFDM resources. As a result of the experiment, the level the time shift and the modulus the impulse response of the input signals for the corresponding receiving antenna were set.

In this case, a shift was recorded in the frequency region of 117 Hz. Synchronization block offset in the time domain: 2,200 samples (0.1432 ms). The cell ID was successfully determined (visualized in Figure 8). In Figure 9 is a plot of the PSS correlation versus frequency offset for a signal-to-noise ratio SNR = -12.5 dB. In this case, a shift was recorded in the frequency region of 11.5 kHz. Synchronization block offset in the time domain: 240,237 samples (15.6404 ms). The cell ID is not defined correctly. The correlation of SSS symbols on the receiver is shown in Figure 10.

When comparing the obtained dependences of the PSS correlations on the frequency offset, the following conclusions can be drawn: for SNR = 15 dB, there is one peak of the strongest correlation for a frequency offset of 0 kHz with a spurious range of 0.044 and an average level of 0.125; for SNR = -12.5 dB, there are three peaks of the strongest correlation for frequency offsets of -45, 0, and 45 kHz, with spurious peak-to-peak values of 0.088 and an average of 0.48. This leads to an error in determining the cell identifier and the impossibility of establishing synchronization between the transmitter and the receiver. That is, outside of the synchronization setting area between the transmitter and the receiver, it becomes impossible to correctly determine the peak of the strongest correlation of the received waveform with each candidate PSS sequence.

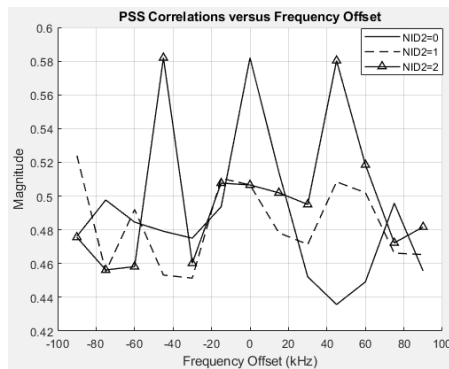


Figure 9. Graphical correlation estimates of PSS versus frequency change (SNR = -12.5 dB)

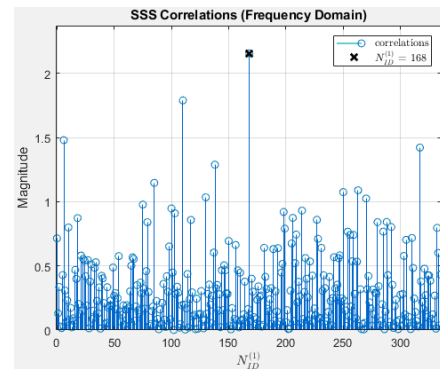


Figure 10. SSS correlation at the receiver (SNR = -12.5 dB)

3.2. Estimation of the root-mean-square value of the magnitude of the error vector

Consider the definition the RMS magnitude of the EVM in the PBCH. We simulated the channel with TDL and changed the SNR level (Figure 11). The studies were carried out for a channel with fading, using multiple input multiple output (MIMO) [3] mode to obtain an attenuated signal.

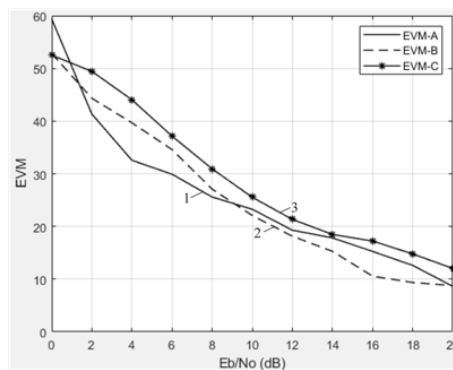


Figure 11. The dependence of EVM on SNR in PBCH for three different channels where 1 is the TDL-A profile; 2 there is a TDL-B profile; and 3 there is a TDL-C profile

For the study, the channel models of the TDL-A, TDL-B and TDL-C types were used, which define the profiles for the structure of the channels without line of sight. The Doppler shift was determined from the formula $f_D = |\bar{v}|/\lambda_0$ [25]. The dependence of EVM on SNR in PBCH for three different channel profiles without line of sight is shown in Figure 11.

From the obtained dependencies, we can conclude that the EVM value for the PBCH channel varies from 55% to 10% when the SNR changes from 0 to 20 dB. The studies were carried out for the frequency bands FR1 (410–7,125 MHz) and FR2 (24.25–52.6 GHz). Our research shows that the design of 5G communications must be a compromise between providing the desired data rate and providing an acceptable EVM.

3.3. Estimate coarse and fine frequency offset when synchronizing

In Figure 12 shows the dependence of the bit error rate (BER) [7] on SNR (E_b/N_0) for the PSS and the PBCH. The frequency offset versus SNR for 5G mobile telecommunications is shown in Figure 13. We focus on the fact that structurally SS is formed by the SSS, PSS and PBCH signals, which occupy the first four OFDM symbols in the resource grid (Figure 4).

Analysis of the obtained results presented in Figure 13 leads to the following conclusion. With decreasing SNR, the fine frequency offset increases exponentially and on the verge of synchronization breakdown, increases by a factor of 1.5. In this case, the displacement in the time domain increases by a factor of 100.

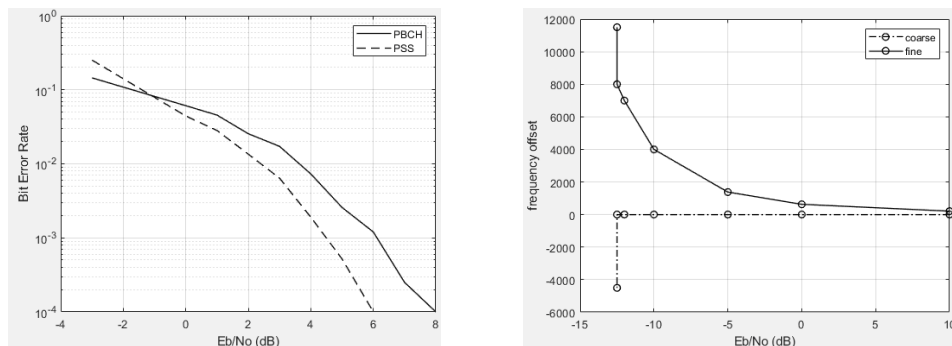


Figure 12. BER versus E_b/N_0 for PSS and PBCH Figure 13. The frequency offset versus SNR

4. CONCLUSION

The article studies the conditions for ensuring synchronization of user means with base station signals. At the stage of connecting to the network, the user means must perform the cell search and selection process and obtain the initial system information. The search for a cell is based on the separation of the PSS and SSS, but the presence of interference in the communication channel introduces certain errors. The cell search procedure requires the accurate detection and elimination of time and frequency offsets in the communication system. The paper analyzes the resource grid formed by the 5G signal, analyzes the synchronization signals, algorithms for cross-correlation and autocorrelation synchronization.

As a result of studying the correlation of the received waveform with each of the three possible PSS sequences, the following results were obtained: for SNR = 15 dB, there is one peak of the strongest correlation for a frequency offset of 0 kHz with a spurious swing of 0.044 and an average level of 0.125; for SNR = -12.5 dB, there are three peaks of the strongest correlation for frequency offsets of -45, 0, and 45 kHz, with spurious peak-to-peak values of 0.088 and an average of 0.48. This leads to an error in determining the cell identifier and the impossibility of establishing synchronization between the transmitter and the receiver. An analytical description of the process of forming physical layer cells ID, the number of which for 5G is 1,008, is presented.




The RMS values of EVM in PBCH versus SNR are investigated. It is concluded that the EVM value for the PBCH channel changes from 55% to 10% when the SNR changes from 0 to 20 dB. It is concluded that the SNR limits for PSS determination may be 2 dB lower than for PBCH determination. Estimated coarse and fine frequency offset in 5G. Analysis of the frequency offset versus SNR suggests that for SNR = 15 dB, the exact frequency offset is 117 Hz. As SNR fine decreases, the frequency offset increases exponentially.

REFERENCES




- [1] A. Omri, M. Shaqfeh, A. Ali, and H. Alnuweiri, "Synchronization Procedure in 5G NR Systems," in *IEEE Access*, vol. 7, pp. 41286-41295, 2019, doi: 10.1109/ACCESS.2019.2907970.
- [2] M. Sawada, Q. N. Nguyen, M. M. Alhasani, C. Safitri, and T. Sato, "OFDM synchronization system using wavelet transform for symbol rate detection," *Telecommunication Computing Electronics and Control (TELKOMNIKA)*, vol. 18, no. 3, pp. 1658-1670,

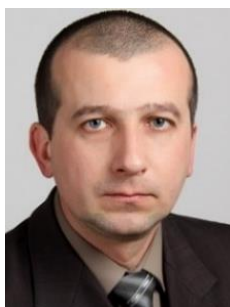
- 2020, doi: 10.12928/telkomnika.v18i3.14834.
- [3] N. Praba and K. M. Ravikumar, "PAPR Reduction at Large Multi-User-MIMO-OFDM using Adaptive Data Detection Algorithm," *Indonesian Journal of Electrical Engineering and Computer Science (IJECCS)*, vol. 12, no. 3, pp. 1071-1080, 2018, doi: 10.11591/ijeecs.v12.i3.pp1071-1080.
 - [4] K. Jaganathan and B. Hassibi, "Reconstruction of Signals From Their Autocorrelation and Cross-Correlation Vectors, With Applications to Phase Retrieval and Blind Channel Estimation," in *IEEE Transactions on Signal Processing*, vol. 67, no. 11, pp. 2937-2946, 2019, doi: 10.1109/TSP.2019.2911254.
 - [5] H. M. Jawad, M. J. A. -AlShaer, S. Yevseiev, V. Kornienko, and O. Turovsky, "Improvement of the Methodology of Building a System of Phase Synchronization of Coherent Demodulators in Telecommunication Control Systems and Distance Learning," *2022 International Symposium on Multidisciplinary Studies and Innovative Technologies (ISMSIT)*, 2022, pp. 1013-1016, doi: 10.1109/ISMSIT56059.2022.9932844.
 - [6] M. Korde, "Synchronization Aspects in 5G," *2020 International Conference on Communication and Signal Processing (ICCSIP)*, 2020, pp. 0474-0478, doi: 10.1109/ICCSIP48568.2020.9182120.
 - [7] J. Boiko, I. Pyatin, L. Karpova, and O. Eromenko, "Study of the Influence of Changing Signal Propagation Conditions in the Communication Channel on Bit Error Rate," *Data-Centric Business and Applications. Lecture Notes on Data Engineering and Communications Technologies*, Switzerland: Springer, Cham, 2021, vol. 69, pp. 79-103, 2021, doi: 10.1007/978-3-030-71892-3_4.
 - [8] Y. He, Y. Gu, S. Bu, and Z. Mao, "Primary Synchronization Signal Design for New Radio Technique in 5G Communication System," in *1st Workshop on Fog Computing-Based Radio Access Networks for 5G*, 2017, pp. 265-269, doi: 10.4108/eai.13-7-2017.2270278.
 - [9] M. I. Youssif, A. E. Emam, and M. A. ElGhany, "Image multiplexing using residue number system coding over MIMO-OFDM communication system," *International Journal of Electrical and Computer Engineering (IJECE)*, vol. 9, no. 6, pp. 4815-4825, 2019, doi: 10.11591/ijece.v9i6.pp4815-4825.
 - [10] S. N. Liyanage and S. A. Senanayake, "Content Caching and Clock Synchronization Assisted Low-Latency Communication in 5G Networks," *2020 5th International Conference on Innovative Technologies in Intelligent Systems and Industrial Applications (CITISIA)*, 2020, pp. 1-6, doi: 10.1109/CITISIA50690.2020.9371822.
 - [11] A. Chakrapani, "On the Design Details of SS/PBCH, Signal Generation and PRACH in 5G-NR," in *IEEE Access*, vol. 8, pp. 136617-136637, 2020, doi: 10.1109/ACCESS.2020.3010500.
 - [12] J. Boiko, I. Pyatin, and O. Eromenko, "Simulation of the Transport Channel With Polar Codes for the 5G Mobile Communication," *2020 IEEE International Conference on Problems of Infocommunications. Science and Technology (PIC S&T)*, 2020, pp. 182-186, doi: 10.1109/PICST51311.2020.9468013.
 - [13] J. B. Doré, R. Gerzaguet, N. Cassiau, and D. Ktenas, "Waveform contenders for 5G: Description, analysis and comparison," *Physical Communication*, vol. 24, pp. 46-61, 2017, doi: 10.1016/j.phycom.2017.05.004.
 - [14] M. Schümgel, S. Dietrich, D. Ginthör, S. -P. Chen, and M. Kuhn, "Optimized Propagation Delay Compensation for an Improved 5G RAN Synchronization," *IECON 2021-47th Annual Conference of the IEEE Industrial Electronics Society*, 2021, pp. 1-6, doi: 10.1109/IECON48115.2021.9589252.
 - [15] G. Soatti *et al.*, "Distributed signal processing for dense 5G IoT platforms: Networking, synchronization, interference detection and radio sensing," *Ad Hoc Networks*, vol. 89, pp. 9-21, 2019, doi: 10.1016/j.adhoc.2019.02.006.
 - [16] S. I. Ojo, Z. K. Adeyemo, R. O. Omowaiye, and O. O. Oyedokun, "Autocorrelation Based White Space Detection in Energy Harvesting Cognitive Radio Network," *Indonesian Journal of Electrical Engineering and Informatics (IJEI)*, vol. 9, no. 4, pp. 834-845, 2021, doi: 10.52549/ijeie.v9i4.3179.
 - [17] E. Hännesson, J. Sellers, E. Walker, and B. Webb, "Network specialization: A topological mechanism for the emergence of cluster synchronization," *Physica A: Statistical Mechanics and its Applications*, vol. 600, 2022, doi: 10.1016/j.physa.2022.127496.
 - [18] L. Berkman, O. Tkachenko, O. Turovsky, V. Fokin and V. Strelnikov, "Designing a System To Synchronize the Input Signal in a Telecommunication Network Under the Condition for Reducing a Transitional Component of the Phase Error," *Eastern-European Journal of Enterprise Technologies*, vol. 1, no. 9, pp. 66-76, 2021, doi: 10.15587/1729-4061.2021.225514.
 - [19] N. Y. Kushnir, P. P. Horley and A. N. Grygoryshyn, "Dynamic chaos in phase synchronization devices," *2005 15th International Crimean Conference Microwave & Telecommunication Technology*, 2005, pp. 346-347, vol. 1, doi: 10.1109/CRMICO.2005.1564936.
 - [20] E. A. Manziuk *et al.*, "Approach to creating an ensemble on a hierarchy of clusters using model decisions correlation," *Przegląd Elektrotechniczny*, pp. 108-113, 2020, doi: 10.15199/48.2020.09.23.
 - [21] P. S. Prabowo and S. Mungkasi, "A multistage successive approximation method for Riccati differential equations," *Bulletin of Electrical Engineering and Informatics*, vol. 10, no. 3, pp. 1589-1597, 2021, doi: 10.11591/eei.v10i3.3043.
 - [22] J. Boiko, O. Eromenko, I. Kovtun and S. Petrashchuk, "Quality Assessment of Synchronization Devices in Telecommunication," *2019 IEEE 39th International Conference on Electronics and Nanotechnology (ELNANO)*, 2019, pp. 694-699, doi: 10.1109/ELNANO.2019.8783438.
 - [23] S. H. R. Naqvi, P. H. Ho, and L. Peng, "5G NR mmWave indoor coverage with massive antenna system," *Journal of Communications and Networks*, vol. 23, no. 1, pp. 1-11, 2021, doi: 10.23919/JCN.2020.000031.
 - [24] J. Boiko, I. Pyatin, O. Eromenko, and M. Stepanov, "Method of the adaptive decoding of self-orthogonal codes in telecommunication," *Indonesian Journal of Electrical Engineering and Computer Science (IJECCS)*, vol. 19, no. 3, pp. 1287-1296, 2020, doi: 10.11591/ijeecs.v19.i3.pp1287-1296.
 - [25] S. S. Hreshee, "Automatic recognition of the digital modulation types using the artificial neural networks," *International Journal of Electrical and Computer Engineering (IJECE)*, vol. 10, no. 6, pp. 5871-5882, 2020, doi: 10.11591/ijece.v10i6.pp5871-5882.
 - [26] H. Fourati, R. Maaloul, L. Chaari, and M. Jmaiel, "Comprehensive survey on self-organizing cellular network approaches applied to 5G networks," *Computer Networks*, vol. 199, 2021, doi: 10.1016/j.comnet.2021.108435.
 - [27] S. Zanafi and N. Aknin, "Analysis of cyclic prefix length effect on ISI limitation in OFDM system over a Rayleigh-fading multipath," *International Journal of Electrical and Computer Engineering (IJECE)*, vol. 11, no.4, pp. 3114-3122, 2021, doi: 10.11591/ijece.v11i4.pp3114-3122.
 - [28] D. Mattera and M. Tanda, "Windowed OFDM for small-cell 5G uplink," *Physical Communication*, vol. 39, 2020, doi: 10.1016/j.phycom.2019.100993.
 - [29] A. E. Dinar, S. Ghouali, B. Merabet, M. Feham, M. S. Guellil and E. K. Hussein, "5G Network Performance by Cell-Edge Servers Optimization Assignment (5GNC-CESOA)," *Procedia Computer Science*, vol. 194, pp. 140-148, 2021, doi: 10.1016/j.procs.2021.10.067.
 - [30] J. Boiko, I. Pyatin, and O. Eromenko, "Design and Evaluation of the Efficiency of Channel Coding LDPC Codes for 5G Information Technology," *Indonesian Journal of Electrical Engineering and Informatics (IJEI)*, vol. 9, no. 4, 2021, doi: 10.52549/ijeie.v9i4.3188.




BIOGRAPHIES OF AUTHORS

Ilya Pyatin    received his diploma of a specialist and a qualification of a radio engineer from the Khmelnytskyi Technological Institute (Ukraine) in 1992. In 1996 he received a PhD degree from the Vinnytsia Polytechnic Institute in the field of radio measurements. Until 2021, he worked as an Associate Professor at the Department of Telecommunications at Khmelnytskyi National University. Currently I work at the Faculty of Computer Engineering of the Khmelnytskyi Professional College of the National University “Lviv Polytechnic” (Ukraine). Scientific research includes issues related to the development of error-correcting coding and synchronization systems for modern mobile telecommunications. He can be contacted at email: ilkhmel@ukr.net.






Julyi Boiko    received his Specialist Degree and a Radio Design Engineer qualification from the Technological University of “Podillya” (Ukraine) in 1998. In 2002 he received a Candidate of Science degree (PhD) at the Institute of Electrodynamics of the National Academy of Sciences of Ukraine in the field of device design and development of methods for measuring electrical and magnetic quantities. In 2015, he received a Doctor of Science degree (D.Sc. in Engineering) at the State University of Telecommunications (Kyiv, Ukraine) in the field of signal reception, synchronization, signal processing in telecommunication systems. Currently, Full Professor of the Department of Telecommunications, Media and Intelligent Technologies, Khmelnytskyi National University (Khmelnytskyi, Ukraine). Research includes issues related to the development of devices for the automation of devices and systems, the theory of coding, synchronization systems, diagnostics and signal processing. He can be contacted at email: boiko_julius@ukr.net.



Oleksander Eromenko    received his Specialist Degree and a qualification of a teacher of physics and basics of computer science at the Kamyanyets-Podilskyi State Pedagogical Institute (Ukraine) in 1997. In 2015 he received a Candidate of Science degree (PhD) at the Khmelnytskyi National University in the field of radio-engineering devices and means of telecommunications. Currently, Associate Professor of Physics and Electrical Engineering Department, Khmelnytskyi National University (Khmelnytskyi, Ukraine). Research includes issues related to the development of devices for measurement and signal processing. He can be contacted at email: yeromenko_s@ukr.net.



Igor Parkhomey    received his Specialist Degree and Radio Engineer qualification from the Kyiv Polytechnic Institute (Ukraine) in 1994. In 1999 he received a Ph.D. degree in technical sciences from the Kiev Polytechnic Institute in the field of system adaptive control design. In 2015, he received his Ph.D. in technical sciences from the State University of Telecommunications (Kyiv, Ukraine) in the development of radar systems. Currently, Professor, Department of Software Engineering, National Aviation University (Kyiv). Research includes issues related to the development of robotic devices, radio monitoring and synchronization systems. He can be contacted at email: i_parkhomey@ukr.net.